

The B_K Kaon Parameter in the $1/N_c$ Expansion ¹

Joaquim Prades^{a)}, Johan Bijnens^{b)}, and Elvira Gámiz^{c)}

^{a)} Centro Andaluz de Física de las Partículas Elementales (CAFPE) and
Departamento de Física Teórica y del Cosmos, Universidad de Granada
Campus de Fuente Nueva, E-18002 Granada, Spain.

^{b)} Department of Theoretical Physics, Lund University
Sölvegatan 14A, S-22362 Lund, Sweden.

^{c)} Department of Physics & Astronomy, University of Glasgow
Glasgow G12 8QQ, United Kingdom.

Abstract

We present work going on calculating the kaon B_K parameter in the $1/N_c$ expansion. The goal of this work is to analyze analytically in the presence of chiral corrections this phenomenologically very important parameter. We present the method used and preliminary results for the chiral limit value for which we get $\hat{B}_K^\chi = 0.29 \pm 0.15$. We also give some analytical indications of why the large N_c prediction of $\hat{B}_K = 3/4$ may have small $1/N_c$ corrections in the real case.

January 2005

¹Invited talk given by J.P. at “Large N_c QCD Workshop”, 5-9 July 2004, Trento, Italy.

1 Introduction

Indirect Kaon CP-violation in the Standard Model (SM) is proportional to the matrix element

$$\begin{aligned}\langle \overline{K}^0 | K^0 \rangle &= -iC_{\Delta S=2} C(\nu) \langle \overline{K}^0 | \int d^4y Q_{\Delta S=2}(y) | K^0 \rangle \\ &\equiv -iC_{\Delta S=2} \frac{16}{3} \hat{B}_K f_K^2 m_K^2\end{aligned}\quad (1)$$

with

$$Q_{\Delta S=2}(x) \equiv 4L^\mu(x)L_\mu(x); \quad 2L_\mu(x) \equiv [\bar{s}\gamma_\mu(1 - \gamma_5)d](x). \quad (2)$$

and $C(\nu)$ is a Wilson coefficient which is known in perturbative QCD at next-to-leading (NLO) order in $a \equiv \alpha_S/\pi$ in two schemes [1], namely, the 't Hooft-Veltman (HV) scheme ($\overline{\text{MS}}$ subtraction and non-anti-commuting γ_5 in $D \neq 4$) and in the Naive Dimensional Regularization (NDR) scheme ($\overline{\text{MS}}$ subtraction and anti-commuting γ_5 in $D \neq 4$). The coefficient $C_{\Delta S=2}$ collects well known functions of the integrated out heavy particle masses and Cabibbo-Kobayashi-Maskawa matrix elements. For comprehensive reviews where these factors and complete details can be found see [2]. The Wilson coefficient $C(\nu)$ is

$$C(\nu) = \left(1 + a(\nu) \left[\frac{\gamma_2}{\beta_1} - \frac{\beta_2 \gamma_1}{\beta_1^2} \right] \right) [\alpha_s(\nu)]^{\gamma_1/\beta_1} \quad (3)$$

where γ_1 is the one-loop $\Delta S = 2$ anomalous dimension

$$\gamma_1 = \frac{3}{2} \left(1 - \frac{1}{N_c}\right); \quad (4)$$

γ_2 is the two-loop $\Delta S = 2$ anomalous dimension [1]

$$\begin{aligned}\gamma_2^{\text{NDR}} &= -\frac{1}{32} \left(1 - \frac{1}{N_c}\right) \left[17 + \frac{4}{3}(3 - n_f) + \frac{57}{N_c} \left(\frac{N_c^2}{9} - 1\right)\right], \\ \gamma_2^{\text{HV}} &= \gamma_2^{\text{NDR}} - \frac{1}{2} \left(1 - \frac{1}{N_c}\right) \beta_1\end{aligned}\quad (5)$$

and β_1 and β_2 are the first two coefficients of the QCD beta function.

The so-called \hat{B}_K kaon parameter defined in (1) is an important input for the unitarity triangle analysis and its calculation has been addressed many times in the past. There have been four main techniques used to calculate the \hat{B}_K parameter: QCD-Hadronic Duality [3, 4], three-point function QCD Sum Rules [5], lattice QCD and the $1/N_c$ (N_c = number of colors) expansion. For a recent review on the unitarity triangle where the relevant references for the inputs can be found see [6]. For recent advances using lattice QCD see [7, 8].

Here, we would like to present work going on determining the \hat{B}_K parameter at NLO order in the $1/N_c$ expansion. That the $1/N_c$ expansion would be useful in this regard was first suggested by Bardeen, Buras and Gérard [9] and reviewed by Bardeen in [10, 11]. There one can find most of the references to previous work and applications of this non-perturbative technique.

Recent related work to the one we will discuss in the following sections can be found in [12, 13] where a NLO in $1/N_c$ calculation of \hat{B}_K within and outside the chiral limit is presented. There, the relevant spectral function is calculated using the ENJL model [14] at intermediate energies while at very low energies and at very large energies the chiral perturbation theory (CHPT) and operator product expansion (OPE) results, respectively, are used. Another calculation of \hat{B}_K in the chiral limit at NLO in the $1/N_c$ is in [22]. There, the relevant spectral function is saturated by the pion pole and the first rho meson resonance –minimal hadronic approximation (MHA). In [23], the same technique as in [22] was used but including also the effects of dimension eight operators in the OPE of the $\Delta S = 2$ Green's function and adding the first scalar meson resonance to the relevant spectral function.

2 Technique

All the details on the X -boson method were given in [13]. In particular, in that reference it was shown how short-distance scale and scheme dependences can be taken into account analytically in the $1/N_c$ expansion. Here, we just sketch the procedure introducing the notation. We want to calculate the two-point function [12, 13]

$$\mathbf{\Pi}_{\Delta S=2}(q^2) = i \int d^4x e^{iq \cdot x} \langle 0 | T \left(P_{\bar{K}^0}^\dagger(0) P_{K^0}(x) e^{i\mathbf{\Gamma}_{\text{LD}}} \right) | 0 \rangle \quad (6)$$

in the presence of the long-distance $\Delta S = 2$ effective action of the Standard Model $\mathbf{\Gamma}_{\Delta S=2}$. After reducing the kaon two-quark densities the two-point function (6) provides the matrix element in (1).

The effective action $\mathbf{\Gamma}_{\Delta S=2}$ reproduces the physics of the SM at low energies by the exchange of a colorless heavy $\Delta S = 2$ X -boson. To obtain it [13], we make a short-distance matching analytically between

$$\mathbf{\Gamma}_{\Delta S=2} \equiv -C_{\Delta S=2} C(\nu) \int d^4y Q_{\Delta S=2}(y) + \text{h.c.} \quad (7)$$

and –in our approach–

$$\mathbf{\Gamma}_{\text{LD}} \equiv 2 g_{\Delta S=2}(\mu_C, \dots) \int d^4y X^\mu(y) L_\mu(y) + \text{h.c.} \quad (8)$$

Where, we have chosen to regulate the long-distance effective action in four dimensions with a cut-off μ_C . These choices are perfectly compatible with keeping

the short-distance scale and scheme independence analytically exact and we believe that at low energies, where the relevant degrees of freedom are not quarks and gluons but hadronic degrees of freedom, are more natural.

As said above, this matching takes into account exactly all the short-distance scale and scheme dependences as well as the choice of evanescent operators. We are left with the coupling of the X -boson long-distance effective action completely fixed in terms of the SM ones

$$\frac{g_{\Delta S=2}^2(\mu_C, \dots)}{M_X^2} \equiv C_{\Delta S=2} C(\nu) \left[1 + a \left(\gamma_1 \log \left(\frac{M_X}{\nu} \right) + \Delta r \right) \right]. \quad (9)$$

The one-loop finite term Δr is scheme dependent

$$\Delta r^{NDR} = -\frac{11}{8} \left(1 - \frac{1}{N_c} \right); \Delta r^{HV} = -\frac{7}{8} \left(1 - \frac{1}{N_c} \right) \quad (10)$$

and makes the coupling $|g_{\Delta S=2}|$ scheme independent to order a^2 . This coupling is as well analytically scale- ν independent at the same order. Notice that there is no dependence on the cut-off scale μ_C —this feature is general of four-point functions which are product of conserved currents [13].

In the procedure described above, one also produces the standard leading and next-to-leading resummation to all orders of the large logs in $[\alpha_S \log(M_W/\nu)]^n$ and $\alpha_S [\alpha_S \log(M_W/\nu)]^n$. And this has been done in the two-schemes described before; namely, NDR and HV.

Once the long-distance effective action $\mathbf{\Gamma}_{LD}$ is fully fixed, we are ready to calculate the relevant matrix element.

$$\begin{aligned} \langle \bar{K}^0(q) | e^{i\mathbf{\Gamma}_{\Delta S=2}} | K^0(q) \rangle &= \langle \bar{K}^0(q) | e^{i\mathbf{\Gamma}_{LD}} | K^0(q) \rangle \equiv -iC_{\Delta S=2} \frac{16}{3} \hat{B}_K q^2 f_K^2 \\ &= \int \frac{d^4 p_X}{(2\pi)^4} \frac{g_{\Delta S=2}^2}{2} \frac{i g_{\mu\nu}}{p_X^2 - M_X^2} \mathbf{\Pi}^{\mu\nu}(p_X^2, q^2) \end{aligned} \quad (11)$$

where q^2 is the external momentum carried by the kaons. The basic object is the four-point function

$$\mathbf{\Pi}^{\mu\nu}(p_X^2, q^2) \equiv i^2 4 \langle \bar{K}^0(q) | \int d^4 x \int d^4 y e^{-ip_X \cdot (x-y)} T(L^\mu(x) L^\nu(y)) | K^0(q) \rangle. \quad (12)$$

At large N_c , this four-point function factorizes into two two-point functions at all orders in quark masses and external momentum q^2 . The disconnected part of the four-point $\Delta S = 2$ function is

$$g_{\mu\nu} \mathbf{\Pi}_{\text{disconn.}}^{\mu\nu}(p_X^2, q^2) = (2\pi)^4 \delta^{(4)}(p_X) 8 q^2 f_K^2 \quad (13)$$

which leads to the well-known large- N_c prediction

$$\hat{B}_K^{N_c} = \frac{3}{4}. \quad (14)$$

At next-to-leading in the $1/N_c$ expansion, one has

$$\hat{B}_K = \frac{3}{4} \left[1 - \frac{1}{16\pi^2 f_K^2} \int_0^\infty dQ^2 F[Q^2] \right] \quad (15)$$

with Q^2 the X-boson momentum in the Euclidean space and

$$F[Q^2] \equiv -\frac{g_{\Delta S=2}^2}{8\pi^2} \lim_{q^2 \rightarrow m_K^2} \int d\Omega_Q \frac{Q^2}{Q^2 + M_X^2} \frac{g_{\mu\nu} \Pi_{\text{conn.}}^{\mu\nu}(Q^2, q^2)}{q^2}. \quad (16)$$

The next point is the calculation of (16). There are two energy regimes where we know how to calculate $F(Q^2)$ within QCD. The first one, it is when $Q^2 \gg 1 \text{ GeV}^2$ while q^2 is kept small since we will have to put it on the kaon mass-shell. In this regime, using the operator product expansion within QCD one gets

$$g_{\mu\nu} \Pi_{\text{conn.}}^{\mu\nu}(Q^2, q^2) = \sum_{n=2}^{\infty} \frac{C_{2n+2}^{(i)}(\nu, Q^2) \langle \bar{K}^0(q) | \mathbf{Q}_{2n+2}^{(i)} | K^0(q) \rangle}{Q^{2n}} \quad (17)$$

where $\mathbf{Q}_{2n+2}^{(i)}$ are local $\Delta S = 2$ operators of dimension $2n + 2$. In particular,

$$\mathbf{Q}_6 = 4 \int d^4x L^\mu(x) L_\mu(x) \quad (18)$$

and

$$C_6(\nu, Q^2) = -8\pi^2 \gamma_1 a \left[1 + a \left[(\beta_1 - \gamma_1) \log \left(\frac{Q}{\nu} \right) + \mathbf{F}_1 \right] + O(a^2) \right] \quad (19)$$

with

$$\mathbf{F}_1 = \frac{\gamma_2}{\gamma_1} + (\beta_1 - \gamma_1) \left[\frac{\Delta r}{\gamma_1} - \frac{1}{2} \right] \quad (20)$$

where the a^2 term was not known before. The finite term \mathbf{F}_1 is order N_c and therefore this a^2 term is of the same order as the leading term. In fact, at the same order in N_c there is an infinite series in powers of a .

For the list and a discussion of the dimension eight operators see [23, 25]. In [23] there is a calculation in the factorizable limit of the contribution of the dimension eight operators. Numerically, the finite term of order a^2 competes with that result when Q^2 is around $(1 \sim 2) \text{ GeV}^2$.

The second energy regime where we can calculate $F[Q^2]$ model independently is for $Q^2 \rightarrow 0$ where the effective quantum field theory of QCD is chiral perturbation theory. The result is known [13, 22] up to order p^4

$$F^\chi[Q^2] = 3 - \frac{12}{F_0^2} (2L_1 + 5L_2 + L_3 + L_9) Q^2 + \dots \quad (21)$$

with F_0 the chiral limit of the pion decay constant $f_\pi = 92.4 \text{ MeV}$.

We still need the intermediate energy region for which we use the large N_c hadronic model described in the next section.

2.1 Large N_c Hadronic Model

Up to this point, all the results are model independent. In particular, we have seen in the previous section that there are two energy regimes which can be calculated within QCD. In this section, we describe a large N_c hadronic model which will provide the full $\Pi_{\text{conn.}}^{\mu\nu}(Q^2, q^2)$ which contains these two regimes analytically.

The large N_c hadronic model we use was introduced in [24]. The basic objects are vertex functions with one, two, \dots two-quark currents or density sources attached to them, referred to as one-point, two-point, \dots vertex functions. These

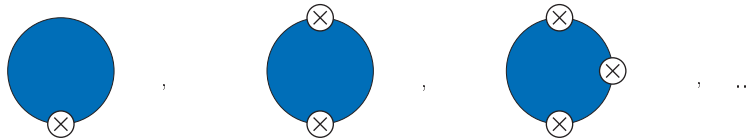


Figure 1: One-point, two-points, three-points, \dots vertex functions. The crosses can be vector or axial-vector currents, scalar or pseudoscalar densities.

vertex functions are glued into infinite geometrical series with couplings g_V for vector or axial-vector sources and g_S for scalar or pseudo-scalar sources. In these way one can construct full n-point Green's functions in the presence of quark masses –see for instance, how to get full two-point functions in Figure 2.

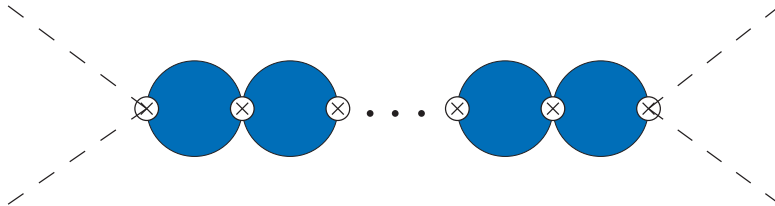


Figure 2: Infinite geometrical series which gives full two-point functions at large N_c . The crosses that glue the vertex functions are either g_V for vector or axial-vector sources or g_S for scalar and pseudo-scalar sources.

The basic vertex functions in Figure 1 have to be polynomials in momenta and quark masses to keep the large N_c structure but just keeping the first octet of hadronic states per channel, i.e., the pseudo-scalar pseudo-Goldstone bosons, the first vectors, the first axial-vectors and the first scalars non-dynamically generated resonances. The coefficients of the vertex functions are free constants of order N_c . Imposing chiral Ward identities on the full Green's functions one can fix most of these unknowns. Chiral perturbation theory at order p^4 and the operator product expansion in QCD help to fix the rest of the free coefficients of the vertex functions.

The full two-point Green's functions obtained from the resummation in Figure 2 agree with the ones of large N_c when one limits the hadronic content to

be just one hadronic state per channel –our model does not produce any less or more constraints and all parameters can be fixed in terms of resonance masses [13]. Introducing two or more hadronic states per channel systematically could be done –it would just be much more cumbersome. To our knowledge, all the low-energy hadronic effective actions used for large N_c phenomenology are in the approximation of keeping the first resonances below some hadronic scale and in some cases not in all channels.

All the process of obtaining full Green’s functions can be done in the presence of quark masses. In fact, in [13] two-point functions were calculated outside the chiral limit and all the new parameters that appear up to order m_q^2 can be fixed except one; namely, the second derivative of the quark condensate with respect to quark masses. Some predictions of the model we are discussing involving coupling constants and masses of vectors and axial-vectors in the presence of masses are

$$\begin{aligned}
f_{Vij}^2 M_{Vij}^2 &= f_{Vkl}^2 M_{Vkl}^2, \\
f_{Vij}^2 M_{Vij}^4 - f_{Vkl}^2 M_{Vkl}^4 &= -\frac{1}{2} \langle \bar{q}q \rangle_\chi (m_i + m_j - m_k - m_l) \\
f_{Aij}^2 M_{Aij}^2 + f_{ij}^2 &= f_{Akl}^2 M_{Akl}^2 + f_{kl}^2, \\
f_{Aij}^2 M_{Aij}^4 - f_{Akl}^2 M_{Akl}^4 &= \frac{1}{2} \langle \bar{q}q \rangle_\chi (m_i + m_j - m_k - m_l), \quad (22)
\end{aligned}$$

where i, j, k, l are indices for the up, down and strange quark flavors.

Three-point functions (see Figure 3) are just calculated at present in the chiral limit – outside the chiral limit three-point functions will be ready soon [26]. Some

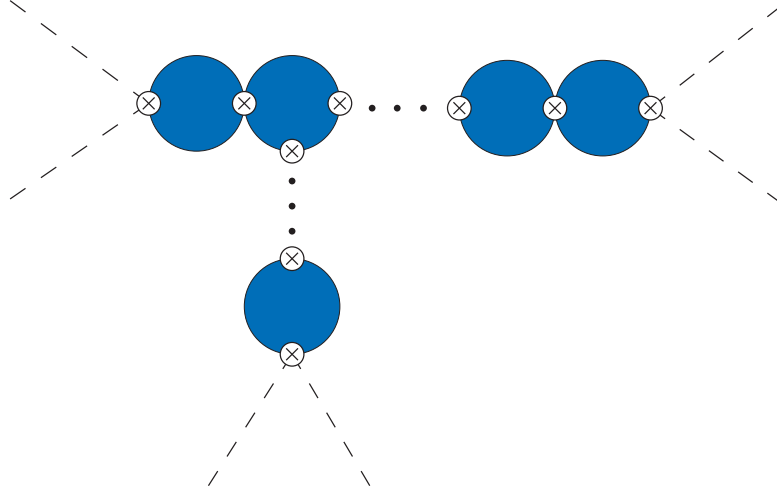


Figure 3: Infinite geometrical series which gives full three-point functions at large N_c . The crosses that glue the vertex functions are either g_V for vector or axial-vector sources or g_S for scalar and pseudo-scalar sources.

three-point functions have also been calculated in other large N_c approaches also

in the chiral limit [15, 16, 17, 18] –for instance, PVV, PVA, PPV and PSP three-point functions, where P stands for pseudoscalar, V for vector, A for axial-vector and S for scalar sources. They agree fully with the ones we get in our model when restricted to just one hadronic state per channel. As we said before one could also add systematically more hadronic states per channel in our large N_c model.

For the moment, we have just calculated the full four-point functions –and the corresponding four-point vertex functions– needed for (12) and in the chiral limit but we are finishing their calculation outside the chiral limit too.

3 Results

After integrating over the four-dimensional Euclidean solid angle Ω_Q and doing the limit $q^2 \rightarrow 0$ as in (16), we get

$$\begin{aligned} F^\chi[Q^2] = & \frac{\alpha_V}{Q^2 + M_V^2} + \frac{\alpha_A}{Q^2 + M_A^2} + \frac{\alpha_S}{Q^2 + M_S^2} + \frac{\beta_V}{(Q^2 + M_V^2)^2} \\ & + \frac{\beta_A}{(Q^2 + M_A^2)^2} + \frac{\gamma_V}{(Q^2 + M_V^2)^3} + \frac{\gamma_A}{(Q^2 + M_A^2)^3}. \end{aligned} \quad (23)$$

This is the input needed in (15) to get \hat{B}_K^χ . The explicit calculation reveals that diagrams with the exchange of vector and axial-vector states produce not only single poles as one may naively assume but two- and three-poles terms in those states masses too. On the opposite, scalar exchange just produce single poles –this is due to the different powers of momenta involved in the scalar vertices with respect to the spin one ones.

The function $F^\chi[Q^2]$ in (16) reproduces the large N_c -pole structure found in [22, 23] but including the first hadronic state in all the channels. The coefficients α_A , α_V , α_S , β_V , β_A , γ_V , and γ_A are known functions of M_V^2 , M_A^2 , M_S^2 , F_0^2 and the four unknowns we mentioned above. We need now to fix these inputs.

For M_V , M_A and M_S , one could either identify them with the measured masses of the corresponding lowest lying hadronic states. That means the first multiplet for the vector and axial-vector multiplet while in the scalar case, the second multiplet is favored in view of the increasing evidence for a dynamical origin of the first –see [19] for a recent discussion of this issue. Another possibility is to use the one to one large N_c relation to write the resonance masses in terms of the order p^4 CHPT couplings L_i . In the large N_c limit both choices are identical. We prefer to take the second strategy since we want to have the order p^4 term in the CHPT expansion exact analytically. We use $L_9 = 5.9 \cdot 10^{-3}$, $L_{10} = -4.7 \cdot 10^{-3}$, $L_5 = 0.9 \cdot 10^{-3}$ from [20, 21] which correspond to $M_V = 0.79$ GeV, $M_A = 1.03$ GeV, and $M_S = 1.43$ GeV, which agree with the experimental masses within the typical $1/N_c$ uncertainty around 30 %.

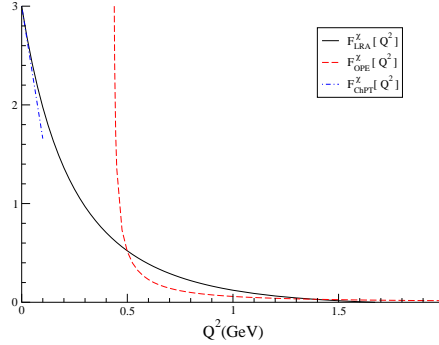


Figure 4: We plot the function $F^x[Q^2]$ in three cases: the full case in (23) is the solid line, the OPE result in (17) is the dashed line and the CHPT result in (21) is the dot-dashed line.

The four unknowns we are left with correspond to three-point functions, namely one for the PSS, one for the PAS and the other two for the PVA three-point function. These we fix as follows: we fix the one related to the PSS three-point function requiring that the slope at the origin is the one in (21); the constant related to the PAS three-point function is fixed by requiring that the residue of the $1/Q^2$ term in the OPE in (17) vanishes. The two constants related to the three-point function PVA are set by requiring at the same time good matching between our $F^x[Q^2]$ and the OPE result including dimension six and eight [23] and that this matching is between 1 and 2 GeV^2 . We checked that the dependence on the exact point of the matching is negligible. That fixes completely all the unknowns.

Notice that we have analytical scale and scheme independence as was explained in Section 2. The result for $F^x[Q^2]$ is plotted in Figure 4.

We now use (15) and integrate (16) up to the matching point μ and from that point on we use the OPE result including dimension eight corrections [23]. This OPE contribution to \hat{B}_K^x is negligible. In Figure 5, we plot the value one obtains for \hat{B}_K^x integrating (16) up to the matching scale μ . Notice the nice plateau one gets between 1 and 2 GeV^2 . Varying all the inputs: values of L_i s needed, α_S , \dots between their respective uncertainties we get as preliminary result

$$\hat{B}_K^x = 0.29 \pm 0.15 \quad (24)$$

which is somewhat smaller but fully compatible with the one found previously also in the chiral limit in [12, 13, 22, 23].

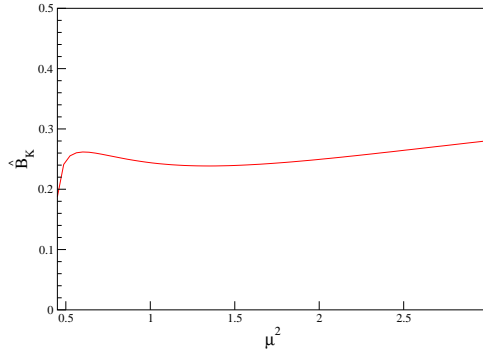


Figure 5: \hat{B}_K^χ plotted vs the upper limit of the integral in (16). See text for further explanation.

4 Prospects and Conclusions

The full analysis of \hat{B}_K including chiral corrections is under way. The results of the two energy regimes explained in Section 2 are known. It is easy to get that $F[0] = 0$ for the real case instead of $F^\chi[0] = 3$ in the chiral limit. Notice that the value of $F^\chi[0]$ is a strong constraint on the value of \hat{B}_K^χ . The CHPT calculation in the real quark masses case $F[Q^2]$ has been done to order p^4 [27] and $F[Q^2]$ remains small –below 0.15– up to energies around 0.2 GeV^2 and then goes negative. The other energy regime in which $F[Q^2]$ is also known is for very large values of Q^2 , which can be calculated using the OPE in QCD. In fact, the dimension six operator and Wilson coefficient are the same as the chiral limit one.

One expects that higher CHPT order terms correct the behaviour of $F[Q^2]$ for $Q^2 > 0.2 \text{ GeV}^2$ and $F[Q^2]$ will tend to the chiral limit curve in Figure 4. The question is at which energy does it happens. This can only be answered using a hadronic large N_c approximation to QCD at present. So, though we have strong indications that the value $\hat{B}_K = 3/4$ has small chiral corrections as shown before, we have to wait till we get the full four-point Green’s function in the real case to confirm it(12).

In the past few years, lattice QCD has produced many calculations using different fermion formulations, including preliminary unquenched studies –see [7, 8] for references. The recommended lattice world average result in [8] is $\hat{B}_K = 0.81^{+0.06}_{-0.13}$. There have also appeared chiral limit extrapolations –like for instance in [28] obtaining $\hat{B}_K^\chi = 0.32 \pm 0.22$ or in [29] obtaining $\hat{B}_K^\chi = 0.34 \pm 0.02$ –which show a clear decreasing tendency with respect to the real case value, in agreement with the results found here and in [12, 13, 22, 23].

The QCD-Hadronic Duality result for \hat{B}_K [3, 4] is very close to the chiral limit result above because –as already mentioned in [4]– what was calculated there, is the order p^2 coefficient of the chiral expansion which actually is the chiral limit

value of \hat{B}_K .

Acknowledgments

J.P. thanks the Department of Theoretical Physics at Lund University where part of his work was done for the warm hospitality. This work has been supported in part by the European Commission (EC) RTN Network EURIDICE Grant No. HPRN-CT-2002-00311 (J.B. and J.P.), by Swedish Science Foundation, by EC Marie Curie Grant No. MEIF-CT-2003-501309 (E.G.), by MCYT (Spain) and FEDER (EC) Grant No. FPA2003-09298-C02-01 (J.P.), and by the Junta de Andalucía Grant No. FQM-101 (J.P.).

References

- [1] A.J. Buras, M. Jamin and P.H. Weisz, Nucl. Phys. B **347** (1990) 491; S. Herrlich and U. Nierste, Nucl. Phys. B **419** (1994) 292; Phys. Rev. D **52** (1995) 6505; Nucl. Phys. B **476** (1996) 27; M. Ciuchini, E. Franco, V. Lubicz, G. Martinelli, I. Scimemi and L. Silvestrini, Nucl. Phys. B **523** (1998) 501.
- [2] A. J. Buras, “Weak Hamiltonian, CP violation and rare decays,” Les Houches lectures 1998, hep-ph/9806471; G. Buchalla, A.J. Buras and M.E. Lautenbacher, Rev. Mod. Phys. **68** (1996) 1125.
- [3] A. Pich and E. de Rafael, Phys. Lett. B **158** (1985) 477.
- [4] J. Prades, C.A. Domínguez, J.A. Peñarrocha, A. Pich and E. de Rafael, Z. Phys. C **51** (1991) 287.
- [5] K.G. Chetyrkin et al. Phys. Lett. B **174** (1986) 104; R. Decker, Nucl. Phys. B **277** (1986) 660; N. Bilić, B. Guberina and C.A. Domínguez, Z. Phys. C **39** (1988) 351; R. Decker, Nucl. Phys. B (Proc. Suppl.) **7A** (1989) 180.
- [6] M. Battaglia et al., hep-ph/0304132.
- [7] M. Wingate, hep-lat/0410008.
- [8] S. Hashimoto, hep-ph/0411126.
- [9] W.A. Bardeen, A.J. Buras and J.-M. Gérard, Phys. Lett. B **180** (1986) 133, Nucl. Phys. B **293** (1987) 787; Phys. Lett. B **192** (1987) 138; Phys. Lett. B **211** (1988) 343; A.J. Buras and J.-M. Gérard, Nucl. Phys. B (Proc. Suppl.) **7A** (1989) 375; J.-M. Gérard, Acta Phys. Polon. B **21** (1990) 257; A.J. Buras in “CP Violation”, C. Jarlskog (ed), World Scientific (1989) p. 575.
- [10] W.A. Bardeen, Nucl. Phys. B (Proc. Suppl.) **7A** (1989) 149.

- [11] W.A. Bardeen in “Kaon Physics”, J.L. Rosner and B.D. Winstein (eds), Univ. Chicago Press (2001), p. 171.
- [12] J. Bijnens and J. Prades, Phys. Lett. **B 342** (1995) 331; Nucl. Phys. **B 444** (1995) 523.
- [13] J. Bijnens and J. Prades, J. High Energy Phys. **01** (2000) 002.
- [14] J. Bijnens, C. Bruno and E. de Rafael, Nucl. Phys. **B 390** (1993) 501; J. Prades, Z. Phys. **C 63** (1994) 491 [Erratum Eur. J. Phys. **C 11** (1999) 571]; J. Bijnens, E. de Rafael and H.q. Zheng, Z. Phys. **C 62** (1994) 437; J. Bijnens and J. Prades, Phys. Lett. **B 320** (1994) 130; Z. Phys. **C 64** (1994) 475; Nucl. Phys. B (Proc. Suppl.) **39BC** (1995) 245; J. Bijnens, Phys. Rept. **265**(1996)369.
- [15] B. Moussallam and J. Stern, hep-ph/9404353; B. Moussallam, Phys. Rev. **D 51** (1995) 4939; Nucl. Phys. **B 504** (1997) 381.
- [16] M. Knecht and A. Nyffeler, Eur. Phys. J. **C 21** (2001) 659.
- [17] V. Cirigliano, G. Ecker, M. Eidemüller, A. Pich and J. Portolés, Phys. Lett. **B 596** (2004) 96.
- [18] P.D. Ruiz-Femenía, A. Pich and J. Portolés, J. High Energy Phys. **07** (2003) 003; Nucl. Phys. B (Proc. Suppl.) **133** (2004) 215.
- [19] V. Cirigliano, G. Ecker, H. Neufeld and A. Pich, J. High Energy Phys. **06** (2003) 012.
- [20] G. Amorós, J. Bijnens and P. Talavera, Nucl. Phys. **B 602** (2001) 87.
- [21] J. Bijnens and P. Talavera, J. High Energy Phys. **03** (2002) 046; Nucl. Phys. **B 489** (1997) 387.
- [22] S. Peris and E. de Rafael, Phys. Lett. **B 490** (2000) 213 [Erratum, hep-ph/0006146].
- [23] O. Catà and S. Peris, J. High Energy Phys. **03** (2003) 060.
- [24] J. Bijnens, E. Gámiz, E. Lipartia and J. Prades, J. High Energy Phys. **04** (2003) 055.
- [25] V. Cirigliano, J.F. Donoghue and E. Golowich, J. High Energy Phys. **10** (2000) 048.
- [26] J. Bijnens, E. Gámiz and J. Prades, in preparation.
- [27] J. Bijnens and J. Prades, unpublished.

[28] W. Lee et al., hep-lat/0409047.

[29] Y. Aoki et al., hep-lat/0411006.